ME-413 - Introduction to additive manufacturing

Project report: M6) Additive processes for glass and crystalline materials

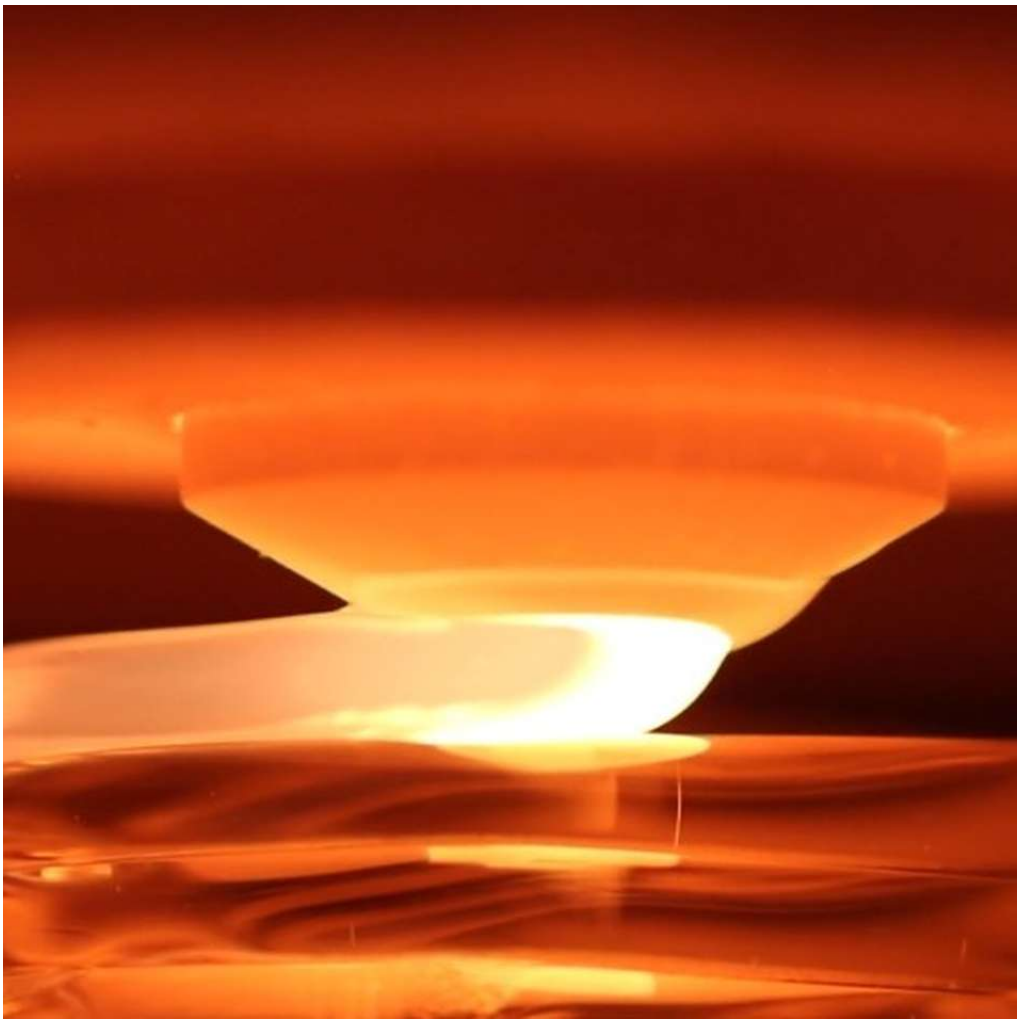

DE FRANCESCO Giandomenico
REINWALT Julian
RICARD Luc
PELISSIER Mathieu

Contents

1 Abstract

This report explores the state of additive manufacturing applied to glass materials, a field that has long remained challenging due to glass's high melting temperature and fragility. We also present the way that microchips composed of silicon are made and how it can be associated with additive manufacturing.

We compare three main additive processes : Fused Deposition Modeling (FDM) and particularly the Glass-3D-Pinted (G3DP) process, Laser Powder Bed Fusion (SLS/SLM), and Stereolithography (SLA) / Digital Light Procesing (DLP). The G3DP process demonstrates the feasibility of printing molten glass directly, achieving transparent and complex geometries suitable for art and architecture. SLS and SLM allow fine control and freedom of form but remain limited by opacity and porosity. Stereolithography provides the highest resolution, particularly for micro-optics, at the cost of complex post-processing.

For the microchips part, we compare micro-fabrication methods such as the Czochralski process, Physical Vapor Deposition (PVD), and Atomic Layer Deposition (ALD). Micro-scale deposition methods such as PVD and ALD, though not conventional additive manufacturing, complement these approaches by enabling atomic-level precision coatings. Together, these techniques highlight the diversity and future potential of additive processes for glass and silicon-based materials in both artistic and technological applications. Each technique is analyzed in terms of working principles, achievable material properties, advantages, limitations, and potential applications.

2 Introduction

Additive manufacturing (AM), commonly known as 3D printing, has opened an entirely new design and manufacturing paradigm. With this method, instead of shaping or removing matter from a block of material, AM creates objects layer by layer. This enables the creation of structures and shapes that were previously impossible.

The origins of additive manufacturing date back to the early 1970s, when Johannes F. Gottwald patented the Liquid Metal Recorder. His idea was to create a continuous inkjet metal device, where the ink is any flowable substance suitable for forming patterns by marking. This is the first patent that describes additive manufacturing with rapid prototyping and controlled on-demand manufacturing of patterns.

Throughout the years, new technologies emerged, including Fused Deposition Modeling (FDM), Laser Powder Bed Fusion (LPBF), Selective Laser Sintering (SLS), Selective Laser Melting (SLM) and Stereolithography (SLA), expanding the range of printable materials to include polymers, metals, and ceramics. Initially limited to prototyping, these processes evolved to become powerful tools for functional and industrial production.

However, glass has remained largely outside the reach of additive manufacturing for many years, despite being a material used by humans for a long time. In fact, the earliest known glass objects come from the Mesopotamia and Ancient Egypt about 4500 years ago. At first it was just created as an accidental byproduct of metalworking. After that, glass making has always been a material for humans to work with. It served to decorate the ancient cathedrals, we made artistic object by glassblowing, as seen in Fig. 1, and also windows for everyday life in an industrial manner.

Historically, glass has always been associated with a balance between craftsmanship and science. Its appeal lies in its transparency, hardness, and resistance to chemical and environmental degradation. Yet, these same properties make it extremely challenging to process. Glass requires high melting temperatures (above 1000 °C) and precise thermal control to avoid cracking. For this reason, even as additive manufacturing became a global research trend in the 2000s, glass remained one of the few materials that could not be easily adapted to additive fabrication.

Figure 1: Object in blown glass. [1]

Research groups began exploring how additive manufacturing could be adapted to glass during the 2010s. Early attempts involved powder-based processes, such as laser sintering or binder jetting, which could form glass-like shapes which were however opaque and porous. In other words, the result was not good.

As seen in figure 2, around 2015, a major breakthrough came from the MIT Mediated Matter Group, led by Neri Oxman, with the development of the Glass 3D Printing Process (G3DP) . This is the first system capable of printing molten glass directly, using a high-temperature extrusion method that fuses layers seamlessly while maintaining optical transparency. Actually, with this FDM method, we can build tall structures, and there are even commercially available systems to buy.

Studies on SLS and SLM in the glass domain also began around 2015. However, the development of these technologies has been very slow as there are difficulties in manufacturing transparent and defect-free objects.

SLA for glass appeared in 2017. Actually, it is still in a research state but there are already promising results in making transparent objects.

As of today, additive manufacturing for glass is still an active research field at the intersection of materials science, design, and digital fabrication. These technologies are not only pushing the boundaries of how glass can be shaped, but also redefining its role as a functional and expressive material.

Given that this technology is so young, there are very few papers and patents on it. Because of this, we decided to enlarge our study to include the manufacturing of microdevices using additive manufacturing. We will talk about the making of parts composed of silicon because it is an important element of glass too.

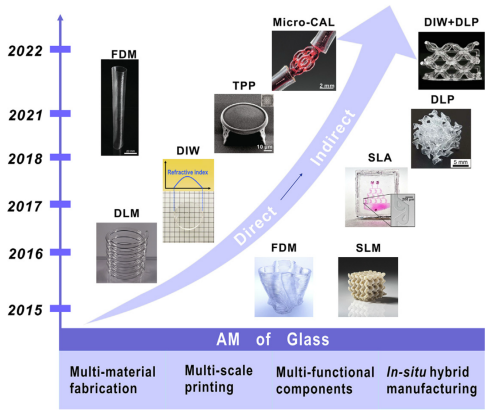

Figure 2: Chronology of additive manufacturing of glass. [2]

The origins of micro-device fabrication come around the early and mid-20th century, when advances in materials science and semiconductor engineering constructed the foundations of the micro-industry. One of the first milestones came in 1916, when Jan Czochralski developed the Czochralski method, a process for growing single-crystal silicon ingots by slowly pulling a seed crystal from molten silicon. This method revolutionized the production of high-purity silicon wafers, which later became the backbone of modern electronics.

During the 1960s and 1970s, the rapid expansion of the semiconductor industry led to the invention of several thin-film deposition techniques designed to precisely control the surface properties of silicon. Among them, Physical Vapor Deposition (PVD) is one of the most widely used methods. In PVD, a material, often a metal or dielectric, is vaporized in a vacuum chamber and deposited as a thin, uniform coating on a substrate.

Later, in the 1990s, the field evolved with the emergence of Atomic Layer Deposition (ALD), which allows the formation of ultra-thin conformal coatings, often just a few nanometers thick, through alternating chemical reactions on the surface.

Although these methods also involve layer-by-layer material addition, they differ fundamentally from traditional additive manufacturing as they operate at the micro- and nano-scale and are used to modify surfaces rather than construct full 3D geometries.

Nonetheless, these historical advances paved the way for today's high-precision fabrication approaches. The ability to control matter at the atomic level through deposition and crystal growth has influenced the evolution of modern additive manufacturing, especially in the development of micro and nanoscale printing.

The goal of this report is to present and compare the main additive manufacturing processes for glass materials, focusing on their principles, capabilities, and limitations. Particular attention is given to the G3DP process, as it remains the most emblematic example of molten glass 3D printing, SLS and SLM, and SLA which are still in the research phase and begin to give interesting results. We will then introduce the Czochralski method, PVD and ALD and compare them.

We structured our research by first searching papers and patents, we then read them and assembled the information found in the different papers to make our report. All our sources can be found a the end of this document.

Giandomenico De Francesco wrote the fused deposition modeling part, Luc Ricard wrote the laser powder bed fusion part, Mathieu Pélissier wrote the stereolithography and Julian Reinwalt wrote the micro devices part.

Part I
Fused deposition modeling

3 Overview of the process

The molten glass additive process works on a principle similar to Fused Deposition Modeling (FDM), where material is extruded through a nozzle and deposited layer by layer to build a 3D structure. However, unlike plastic extrusion, which happens at 200–300 °C and solidifies almost instantly, molten glass printing operates at extreme temperatures above 1000 °C. At this range, glass becomes viscous like honey and needs to be handled carefully, since it does not solidify immediately. Controlling molten glass is much more complex than working with plastics, and the glass flow is driven only by gravity, not by a motor. As the crucible empties, the pressure decreases, which causes the flow rate to slow down and slightly changes the thickness of each deposited filament. The material can also stick to the nozzle edges due to surface tension, creating small irregularities in the print. In addition, the whole system must remain perfectly stable at over 1000 °C, which puts heavy stress on the furnaces and refractory materials and requires a constant energy supply.

To make this possible, the G3DP process developped by the MIT uses a system of three temperature zones. The raw glass is melted in the crucible kiln, stabilized in the nozzle kiln to control viscosity and flow, and deposited inside the annealing kiln, where the printed object cools gradually to prevent cracks caused by thermal stress. This combination of high-temperature melting, viscosity control, and annealing is what allows the creation of transparent, crack-free glass.

We will present this method based on one of their papers [3] and the patent [4] of the G3DP method.

4 Hardware of the G3DP system

The hardware of the G3DP system is built around a stacked structure of three main kiln: the crucible kiln, the nozzle kiln, and the annealing kiln, as seen in figure 3. Each of these zones is made of high-temperature refractory materials, mainly alumina–silica composites, which provide both insulation and structural stability

The crucible kiln, located at the top, contains the raw glass. It is essentially an 1800 W high-temperature furnace made of alumina–silica fiberboard, where the glass is melted and maintained at a temperature of 1040–1165°C. Furthermore, thanks to thermocouples, the temperature is monitored and can be adjusted.

The nozzle kiln is mounted just under the crucible and provides 300 W of heating to the nozzle. The overall structure of the nozzle kiln is similar to that of the crucible kiln. The main difference is that this one features faster response thermocouples to better adapt the temperature. The nozzle itself is machined from bulk high-temperature alumina bisque ceramic rods and is the heart of the system, as even a few degrees of temperature change can affect the flow rate and layer uniformity.

The annealing kiln maintains a temperature above the glass transition temperature of 480–515°C. The print annealer remains stationary while the printing platform moves inside it. The printing platform is fabricated out of a ceramic kiln shelf that enables good initial bonding at high temperature and release at annealing temperature.

The displacement of the printing platform and the nozzle is made thanks to three independent stepper motors and the flow of the melted glass is operated by gravity. This needs to be well controlled to achieve a good print; this will be explained in the next section.

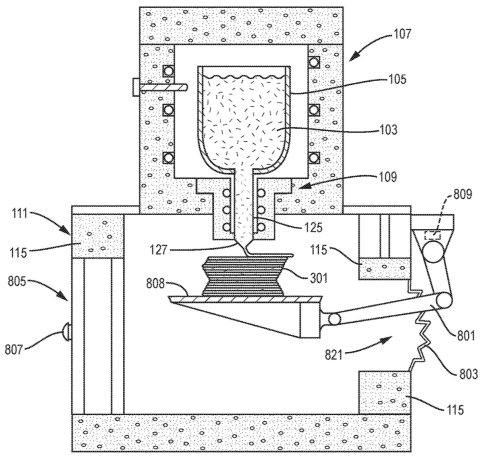

Figure 3: Overview of the G3DP setup [4]

5 Deposition and Control

The deposition step in molten glass printing works on a similar principle to extrusion-based 3D printing for plastics. A controlled stream of molten glass flows out of the nozzle and is deposited layer by layer while the platform and nozzle move. Just like in polymer FDM, the flow follows a programmed toolpath so that the glass filaments stack up to form the object's geometry.

The main difference comes from the material behavior. With plastics, the filament is pushed mechanically and cools almost instantly when it touches the layer below. With glass, the flow is driven by gravity and its viscosity depends entirely on temperature. If the nozzle is too hot, the glass will flow too quickly and if it is too

cool, the flow will slow down or stop.

To maintain precision, the printer synchronizes the two upper kiln's horizontal motion (x–y) with the vertical rise of the printing platform (z), ensuring that each filament has a consistent thickness of around 4–5 mm. Thermocouples continuously monitor the temperature, while parametric software generates smooth, continuous toolpaths that minimize overlaps and abrupt changes in flow.

Throughout the process, the entire printed object remains inside the annealing chamber. This keeps the previously deposited layers warm as new molten glass is added on top, preventing thermal shock and cracking, as seen in figure 4.

In short, the deposition is similar in logic to plastic extrusion but relies on gravity and thermal control instead of mechanical feeding and rapid cooling.

In the next section, we will see why it is so important to control the temperature.

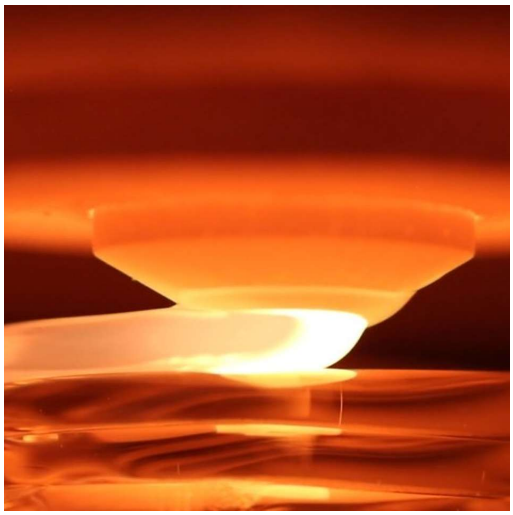

Figure 4: Molten glass flowing inside of the annealing kiln [5]

6 Importance of the temperature control

The thermal field is one of the most critical aspects of molten glass printing. In plastic 3D printing, temperature management is relatively simple: the nozzle melts the polymer, it is extruded, and then it cools and solidifies in seconds. With glass, however, the story is very different because the material remains extremely hot and viscous for a long time.

When the glass leaves the nozzle, it is still at about 920–990 °C. As soon as it is deposited, it begins to cool, which increases its viscosity, so the glass becomes thicker and more resistant to flow. This change is actually helpful: the lower layers solidify just enough to support the next ones, while the upper layers remain

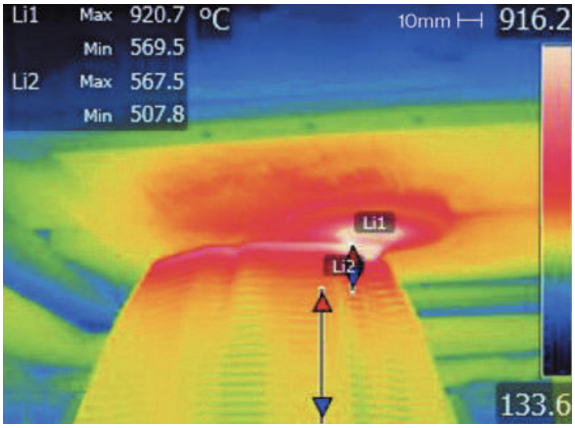

Figure 5: Temperature gradient of an object being printed.[3]

fluid for deposition. In other words, the cooling creates a natural stability in the structure. Simulations show that there is a temperature difference of about 350 °C between the hottest top layers and the cooler bottom of the piece, as seen in figure 5. This gradient is carefully maintained to keep the object stable without causing cracks. To achieve this, the entire printing process takes place inside the annealing chamber, which provides a warm environment that prevents sudden cooling and thermal shock.

The flow of the glass inside the nozzle is also very particular. Because the material is so viscous and moves slowly, the flow is laminar. This means its behavior can be predicted quite well using fluid mechanics equations. However, small changes in temperature or nozzle geometry can have a significant impact on the flow rate, which can cause defects in the printed object.

The combination of precise nozzle temperature control and a stable annealing environment results in improved mechanical and optical properties of the printed object, as will be discussed in the following section.

7 Properties and post-processing

7.1 Properties of 3D printed glass parts

To evaluate the mechanical properties of the printed glasses, different tests were carried out on two types of samples. The first one did not undergo an annealing treatment, and the second one did. The goal was to understand how the annealing process affects the strength and fracture behavior of the material.

The first test was conducted to investigate the presence of residual stresses in the printed samples. Using polariscopy, it was shown that both samples did not have significant stress concentration along the layers. However, looking at the cross section, we can see that printing at room temperature generated radial stresses within layers which the annealed process did not pro-

duce.

The second test was a bending test where the samples were loaded along the layers, which is usually the most critical test for a 3D-printed object. The results show that the annealed sample has a flexural strength that is five times higher than the other one. In both cases, the fracture occured exactly between two layers. These tests show that we can have good mechanical properties due to the annealing process but that the parts are still fragile.

Due to an overall high degree of homogeneity and good adhesion between layers, the light transmission has very little distorsion. When we polish with cerium oxide in both top and bottom layers; a high degree of transparency could be observed by looking above the object. However, if we don't polish them, light refraction and scattering as well as the production of highly complex caustic patterns appears. Furthermore, the layers of about 4 millimeters deform the light transmission when looking from the side of the object.

With these optical properties, we can say that this technique is more adapted to an art or architecture application than doing windows for a house for example.

7.2 Post-processing

The parts coming out of this printer do not really need post-processing. In fact, the annealing is already done and the object is ready to use. However, the layer-by-layer deposition leaves subtle surface undulations (4–6 mm filaments). If a perfectly smooth or optical-grade finish is required, the surface can be mechanically polished using fine abrasives or chemically etched. This step removes surface irregularities and increases transparency.

8 Application Domains

- **Architecture and structural design:** The G3DP process opens completely new possibilities for architectural glass components. Because it can produce freeform, self-supporting geometries, it enables the fabrication of curved walls, domes, columns, or light-diffusing panels that were previously impossible to make using traditional techniques. The printed structures can serve both aesthetic and functional purposes, for instance as translucent façades, daylighting elements, or decorative partitions. The ability to control local thickness and internal geometry also allows architects to integrate structural strength and interesting optical characteristics.

- **Lighting and interior design:** The interplay between geometry and light makes G3DP particularly attractive for lighting applications. By adjusting the shape and pattern of the printed filaments, designers can produce glass lampshades, luminaires, or art installations that project unique caustic patterns on walls and surfaces. The technique allows precise control of how light is refracted, diffused, or concentrated, creating highly customized and dynamic lighting atmospheres. Artists and designers can use G3DP to explore new forms of expression that combine the fluid aesthetics of molten glass with the complexity of algorithmic design. The visible deposition lines can be embraced as part of the artistic language, as seen in figure 6.

Figure 6: Caustic patterns created by illumination from a suspended overhead LED.[3]

- **Scientific and experimental applications:** Beyond design and art, G3DP offers potential in research and material science, especially for studying glass solidification, thermal gradients, or additive manufacturing processes under extreme temperatures. It can also serve as a platform for developing new glass compositions and testing how their optical and mechanical properties evolve under additive fabrication conditions.

9 Advantages and limitations

9.1 Advantages

- **Design freedom:** G3DP allows the creation of complex, freeform geometries and internal cavities impossible to achieve with blowing, casting, or molding.

- **Repeatability:** Especially in art application, glass

objects are usually hand-made and they are not always the same. With this technology, each piece is printed directly from a 3D model, ensuring perfect reproducibility and dimensional accuracy.

- **Less waste:** This technique eliminates the need for single-use molds, reducing material waste and setup time.
- **Easy configuration:** This technique uses G-code from CAD design as all the other 3D printers. This allows the user to easily design its part and send the G-code to the printer thanks to a slicer
- **Controlled cooling:** With the annealing kiln, we can assure better cooling to prevent stress concentration. This allows parts to be less fragile.

9.2 Limitations

- **Technical complexity:** The process requires maintaining three independent thermal zones at precisely controlled temperatures, sometimes exceeding 1100 °C. Managing such conditions demands specialized refractory materials, precise sensors, and automated regulation systems, which make G3DP technically challenging. Furthermore, the repairs can be difficult because the parts are really specific.
- **Resolution:** The extrusion process leaves visible layer lines about 4-6 mm wide. Although the surface is smooth to the touch, it retains a wavy texture that may affect optical perfection. Traditional glassblowing and molding naturally produce seamless, mirror-like surfaces.
- **Slow production rate:** Each layer of glass must be extruded, cooled, and stabilized before the next one is added. Depending on the part's size, printing can take several hours, whereas a skilled glassblower or casting process could produce similar objects in minutes. This makes the method unsuitable for mass production.
- **High energy consumption:** Keeping multiple furnaces above 1000 °C for long durations consumes large amounts of energy. Industrial glassmaking, while also energy-intensive, benefits from continuous production lines that are more efficient per unit of output.
- **Thermal sensitivity:** Even a minor temperature fluctuation or change in glass level within the crucible can alter flow rate, layer thickness, or viscosity. Maintaining a perfectly stable process over hours of continuous printing is technically demanding and prone to interruptions.

10 G3DP2

The G3DP2 is an evolution of the G3DP presented in 2017. This new manufacturing platform has a digitally integrated thermal control and a new four-axis motion-control. With these modification, the flow control, the spatial accuracy and the precision is better. Furthermore, it allows a faster production time and a continuous deposition of up to 30kg of molten glass. With this new machine, they presented at the 2017 Milan Design Week 3 meter-tall columns, made of several stacked parts, fully manufactured with the G3DP2, as seen in figure 7. However, like the first iteration, this printer is not available to purchase.[6]

11 Other available printer in the industry

Another company called Maple Glass Printing builds and actually sells a 3D printer for glass using FDM. They sell the printer in two parts, the Maple 4 that actually print and the Vitri-Glass 2, that produces the filament by melting glass. The total price of this machine is 45'000 USD.[7]

Figure 7: 3 meter-tall columns at the Milan Design Week made with G3DP2.[6]

Part II
Laser Powder Bed Fusion

12 Overview of the process

Laser Powder Bed Fusion (LPBF) is an additive manufacturing term that encompasses two main techniques: Selective Laser Sintering (SLS) and Selective Laser Melting (SLM). Both rely on the same approach: a laser heats a powder feedstock to produce parts layer-by-layer, although in SLS, the laser only heats the powder enough to fuse the particles together without fully melting them, which is called sintering, whereas SLM uses higher laser energy to completely melt the powder, allowing it to solidify into a fully dense part once cooled. Both approaches are now being explored for glass fabrication, and the following sections present recent advances in each field based on various studies in the field.

The process begins with a 3D model created using computer-aided design (CAD) software. This digital model is sliced into thin horizontal layers, each corresponding to a cross-section of the final part.

Inside the machine, a recoater spreads a thin and uniform layer of glass powder over the build platform, a high-power laser then scans the surface according to the geometry of the current layer, locally sintering/melting the powder where material is required. The unsintered/unmelted surrounding powder remains loose and acts as a support for the part during fabrication. Once a layer is completed, the build platform lowers by one layer thickness, a new layer of powder is deposited, and the laser scanning process repeats until the entire part is formed.

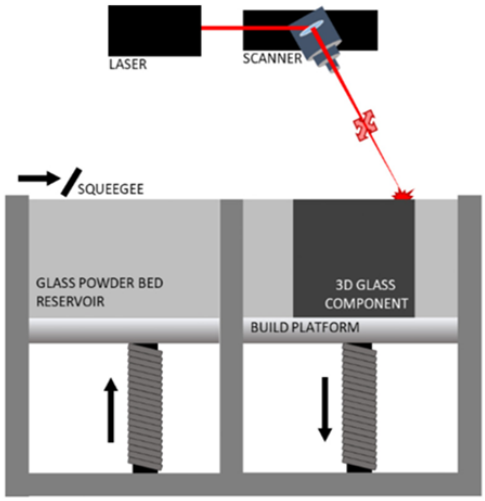

Figure 8: Overview of the LPBF setup [8].

However, applying LPBF to glass introduces specific challenges that need to be addressed in order to successfully produce glass parts. These challenges are discussed in the following sections.

13 Material Requirements and Process Parameters

13.1 Feedstock requirements

The selection of a suitable feedstock is one of the most critical aspects for successfully making glass through LPBF. The material must be chemically compatible with the process, possess appropriate particle shape, size and flowability, and exhibit good thermal and optical behaviour to ensure consistent layer deposition and effective laser absorption.

The glass composition directly governs its melting temperature, viscosity, and crystallization tendency during laser exposure. Among various glass powders tested in research, soda-boro-silicate (silica (SiO_2), boron oxide (B_2O3), sodium oxide(Na_2O)) glass has emerged as one of the most suitable candidates for SLS [8], [9] as it has a low thermal expansion (4-5 $\times 10^{-6} K^{-1}$ for the temperatures achieved for sintering of glass) and is resistant to thermal shock. It is not used for SLM as its melting point is too high ($\approx$ 1650°C) [10]. For SLM soda-lime silica glass (SLG) (silica (SiO_2), soda (Na_2O), and lime (CaO)) has been preferred [11], [12] because its melting temperature ($\approx$1400°C) is more easily achievable with current SLM systems, it exhibits a stable viscosity-temperature relationship and good chemical stability. Moreover, its widespread industrial use makes it a logical choice for process development [13].

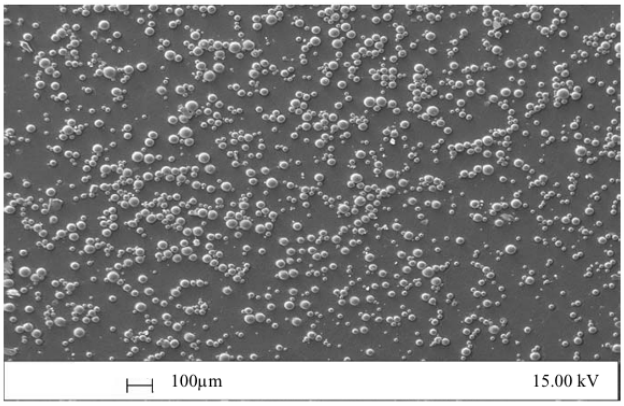

Figure 9: SEM image of glass powder [12].

Particle size and morphology play an important role in determining the quality of the glass produced by this technique. In the experiments performed, particle size varies from 1 to 150 μm but most of them have shown that relatively fine powders with high packing density (volume occupied by solid particles/total volume of the powder bed) are generally better in LPBF as

they provide a larger surface area for laser processing and minimize porosity in the built parts [8], [11], [14]. However, too fine a powder can also cause difficulties with flow, deposition and spreading of the powder over the build [15]. As for the particle shape, most studies use spherical particles since in classical LPBF they improve flowability and therefore powder deposition [16], [11], [17]. However, this topic requires further investigation, as a recent study by Yang et al. (2023) [18] demonstrated that irregularly shaped soda-lime silica glass powder can also be successfully used in SLM of glass. By optimizing the process parameters, builds with porosity comparable to those obtained using typical spherical powder were achieved.

Finally, the low absorptivity of both the glass powder and the glass substrate is a crucial parameter to consider. For the powder to sinter or melt, it must efficiently absorb the energy provided by the laser. In the experiments conducted by Datsiou *et al.* (2021) [11] with an yttrium fibre laser operating at a wavelength of 1064 nanometer, it was shown that the poor absorption of the glass powder caused part of the laser irradiation to reach the surface of the titanium base plate beneath the glass substrate. Some of this irradiation was subsequently reflected and re-directed to the glass substrate, etching its lower surface (Fig. 10 (a)). To prevent this, a less reflective aluminum base plate was used (Fig. 10 (b)). Since aluminum has a higher thermal resistance than glass and similar thermal expansion coefficients, it helps prevent the formation of microcracks that tend to occur when using a glass substrate, while still providing adequate adhesion to the glass [11]. In the experiments conducted by Koppka *et al.* (2023) [8], where a CO_2 laser with a 10600 nanometer wavelength was used, a black base was used as the same problem applies for soda-borosilicate glass powder.

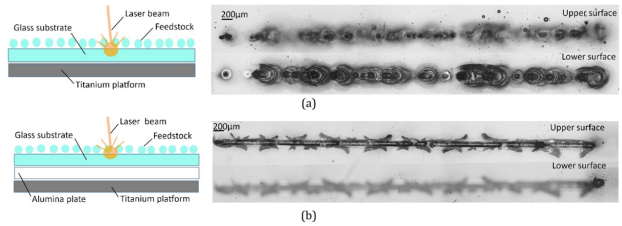

Figure 10: Micrographs of the upper and lower surface of single scan tracks (SLSG109 powder, 100 W and 37 mm/s) formed on a soda lime silica glass substrate that is fixed to (a) a titanium platform and (b) an alumina plate [11].

13.2 Process Parameters

The feedstock requirements are only one part of the highly demanding conditions needed to process glass with LPBF, there are also process parameters that define the success of the process, the most important ones are : laser power, scan speed, hatch spacing and layer thickness.

These parameters are all closely linked by the surface or volumetric energy density given by the formula:

$$ED_{2D} = \frac{P}{v \cdot t} \qquad \text{and} \qquad ED_{3D} = \frac{P}{v \cdot h \cdot t} \quad (1)$$

where ED_{2D} and ED_{3D} are the surface and volumetric energy densities, respectively, P is the laser power (W), v is the scan speed (mm/s), h is the hatch spacing (mm), t is the layer thickness (mm).

For SLS and SLM for thin-walled structures, a surface energy density is used, as it better represents the process where the particles are only partially melted or sintered at the surface to form necks between adjacent grains. For SLM of thick-walled structures, a volumetric energy density is used as they involve multiple and adjacent laser scans per layer.

For SLS, the experiment carried out by Koppka *et al.* (2023) [8], a surface energy density between 0.4 and 0.6 J/mm^2 results in the formation of a stable glass layer , whereas for the experiment for SLM by Datsiou *et al.* (2021) [11], experiments showed that thin-walled glass structures require a volumetric energy density of 20-30 J/mm^2 to achieve melting and consolidation of the powder . In the case of thick-walled structures with SLM, the process window shifts to 65-110 J/mm^3 [11]. Energy densities below these ranges result in poor consolidation and brittle parts, whereas excessively high values cause balling, a phenomenon where the molten glass becomes unstable and breaks into small spherical droplets, leading to discontinuous melt tracks and rougher surfaces. This, in turn, results in excessive track height and poor dimensional accuracy as shown in Fig. 11.

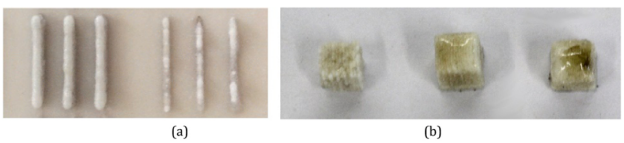

Figure 11: LPBF of glass: (a) Thin walled structures showing good consolidation (left) and poor consolidation (right) and; (b) cubic structures showing poor consolidation (left), good consolidation (middle) and balling (right) [11].

For SLM, in the experiments carried out by Fateri et al. (2014) [12], optimum process parameters for single layers were found to be for a laser power of 60 W, a scan speed of 67 mm/s and a layer thickness of 150 μm which translates to a surface energy density of 6 J/mm^2.

Other parameters to consider also exist, such as the laser spot size, which directly affects the energy concentration and resolution of the melt tracks. For SLS, in Koppka *et al.* (2023) [8] the laser spot size was 220

μm. For SLM, in Datsiou et al. (2021) [11], the fiber laser had a spot diameter of 20 μm, while in Fateri et al. (2014) [12], the Nd:YAG laser used exhibited a larger beam diameter of approximately 200 μm, which reduced precision but allowed for a better bonding between the particles.

Finally, the process of LPBF induces significant thermal gradients, especially when processing glass due to its low thermal conductivity. To reduce these gradients, the temperature of the build platform is maintained at a high temperature (typically around 250°C or even higher) during fabrication using an integrated heater [11].

14 Microstructure, Results and Properties

14.1 Process Results

The glass parts manufactured with laser powder bed fusion are opaque as shown in Fig. 15, Fig. 16, Fig. 17. This is attributed to the presence of superficial, partially fused powder particles and internal defects. For SLS, according to the research done by Koppka *et al.* (2023) [8], cubes fabricated at optimum process parameters showed good macroscopic stability but were brittle and opaque. They could be handled without disintegration, but no translucency was observed due to the remaining porosity and insufficient densification (Fig. 12). Analysis of the structure revealed the presence of partially fused particles with distinct neck formation. Pores between particles remained visible, confirming incomplete melting and a porous microstructure which is what was to be expected with selective laser sintering.

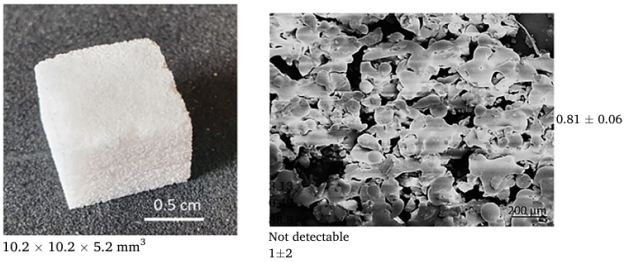

Figure 12: Nano-porous SLS cuboid: global structure (left) and detailed microstructure (right) [8].

In the case of SLM, according to Datsiou *et al.* (2021) [11], the parts obtained are also opaque. A micro-CT analysis of fabricated cubic structures (Fig. 13)) revealed the presence of pores, cracks, and areas with unsintered powder particles randomly distributed within the glass parts Fig.(mettre numéro). Cracks, mainly located near the substrate, are attributed to thermal stresses caused by temperature gradients during processing, and could be reduced by increasing the platform temperature. Finally, semi-fused surface particles ("satellites") and internal defects can be seen in the parts, they contribute to the opaque appearance of the parts.

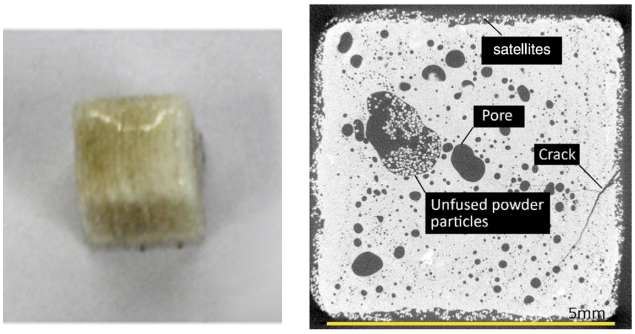

Figure 13: Cubic structure with good consolidation (left) and CT slice of glass cube containing typical defects (pores, cracks and unfused powder particles) (right) [11].

In terms of achievable resolutions, SLS demonstrated the ability to produce single tracks and thin-walled structures with scan line spacings down to about 50 µm and stable 3D geometries as small as 2 mm in size [8]. The process, however, remains limited by partial sintering, which restricts the formation of finer features and leads to inherently porous and brittle parts. As for SLM, it achieved consolidated geometries with higher dimensional control, producing hollow channels as small as 1.1 mm in internal diameter and up to 14 mm in length for thin walls (0.2 mm) before cracking occurred [11]. Although deviations between designed and manufactured dimensions were observed (wall thickening up to 200%), the SLM process allows for finer, more continuous features than SLS due to complete melting and improved densification.

14.2 Mechanical Properties

Mechanical tests are also crucial, as they provide quantitative insight into the strength and reliability of the fabricated glass parts. For SLM, Datsiou *et al.* (2021) [11] performed flexural strength tests (Fig. 14) and results showed that the mean flexural strength of the printed parts ranged between 6.2 and 6.9 MPa, which is 10 to 15 times lower than that of conventional soda-lime glass. This reduction was attributed to the internal porosity, which slightly exceeded 10%, creating stress concentration sites that triggered early fracture.

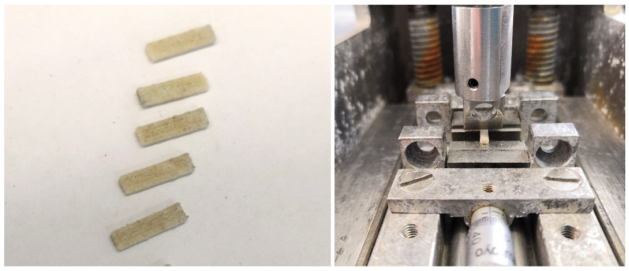

Figure 14: 3-point bending test: (a) samples and (b) set-up [11].

For SLS, no mechanical tests were performed in currently existing experiments, however, the produced parts were qualitatively described as very brittle due to incomplete densification [8].

15 Applications and Developments

15.1 Applications

The glass parts produced with LPBF are opaque and even though transparency is desirable, there are applications where the need for geometrical complexity in combination with chemical inertness is more crucial. In particular, for continuous flow reactor (Fig. 15) and structure catalysts applications (Fig. 16 and Fig. 17), the chemical inertness of glass surpasses the need for transparency. The presence of partially fused powder particles on the walls could be beneficial in such applications as they improve mixing of reactants in continuous flow reactors or increase the surface area in structured catalysts. Additionally, the presence of porosity is not expected to affect their performance as pores were found to be fully enclosed indicating that a leak tight performance is possible for continuous flow reactors. Even though the mean flexural strength of the additively manufactured parts was found to be significantly lower than standard float glass, this is expected to be sufficient for low pressure applications.

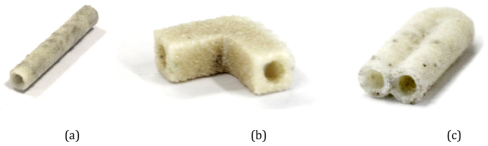

Figure 15: Continuous flow reactor channels: (a) linear cylindrical channel (10 mm length and 2 mm internal diameter), (b) angle channel (12.5 mm length/side and 3 mm diameter) and (c) U-shaped channel (10 mm length and 2 mm internal diameter) [11].

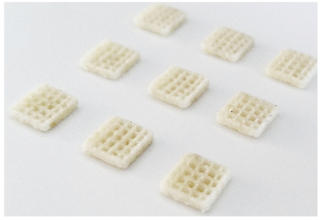

Figure 16: Structured catalyst example: grid shaped rectangles ($7 \times 7 \times 1mm^3$) [11].

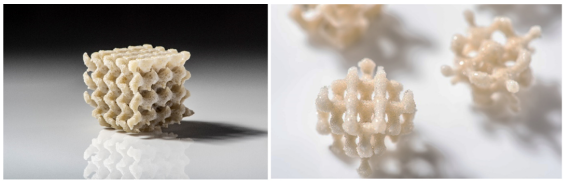

Figure 17: Structured catalyst examples: Gyroid network lattice ($20 \times 20 \times 20mm^3$) (left), and diamond network and BCC lattices ($10 \times 10 \times 10mm^3$) (right) [11].

15.2 Developments

Recent research efforts are increasingly focused on overcoming the current limitations of LPBF for glass by improving densification. One promising direction lies in the development of new glass compositions or doped formulations with enhanced laser absorptivity and lower viscosity in the molten state, enabling better flow and bonding between particles. Further progress can also be achieved through the combination of LPBF with post-processing treatments, such as annealing to relieve internal stresses, secondary sintering to increase density, or mechanical and chemical polishing to improve optical quality. The ultimate objective of these developments is to achieve fully dense and transparent glass parts fabricated directly by LPBF, bridging the gap between additive and conventional glass manufacturing technologies.

16 Advantages and Limitations

16.1 Advantages

- **Design freedom and complexity:** LPBF can produce complex shapes like internal channels and lattices that are impossible or very expensive to mold or machine.
- **Customization and rapid prototyping:** Geometries can be modified directly from CAD data, reducing the cost for low-volume or research applications.
- **Chemical inertness retained:** Despite being opaque, the parts maintain the intrinsic chemical resistance and thermal stability of glass, making

them suitable for chemical or pharmaceutical uses where transparency is not critical.

- **Potential for functional surface textures:** The naturally rough surface and partially fused particles can enhance mixing or catalytic activity in flow applications.

16.2 Limitations

- **Optical opacity and porosity:** The parts remain opaque because of residual pores and incomplete densification, far from the transparency of conventional fused or cast glass.
- **Low mechanical strength:** Even in optimized conditions, the flexural strength (6-7 MPa) is 10 to 15 times lower than that of conventionally produced glass (around 100 MPa).
- **Thermal stresses and cracking:** High temperature gradients during laser exposure induce cracking, requiring substrate pre-heating and careful parameter control.
- **Surface roughness and accuracy:** Semi-fused powder and heat-affected zones lead to dimensional deviations and surface irregularities.
- **Limited scalability and high energy demand:** The process has so far only been able to produce small-scale parts, typically on the order of a few centimeters at most, and it remains highly energy-intensive.

Part III
SLA - DLP

17 Overview of the process

The principle of creating glass objects through stereolithography is an indirect, multi-stage process that transforms a custom resin (photoresist with silica particles) into a pure glass object. It begins with the photoresist being loaded with fine silica particles which is the primary component of glass. A stereolithography (using a UV laser) or Digital Light Processing (DLP, using a UV projector) printer uses a UV light source to selectively solidify this resin layer by layer, building a three-dimensional object known as the "green part." At this stage, the object possesses the correct geometry but is not yet a glass part and fragile, as it consists of silica powder held together by a polymer matrix.

The post-processing stages are critical for achieving the desired glass part. The green part is first placed into a furnace for a thermal treatment called debinding, where it is heated to a medium temperature to slowly and completely burn out the polymer binder. What remains after this step is a porous and fragile silica structure called the "brown part," which retains the shape but is still only silica particles slightly bound together. The final step is sintering, where the brown part is heated to a very high temperature, approaching the melting point of glass. During sintering, the silica particles fuse together at their boundaries, densifying the entire structure into a solid, pore-free, and transparent glass object. In this method the additive process acts as a precise shaping tool for a polymer lost pattern, while the thermal post-processing performs the transformation to create the final solid glass.

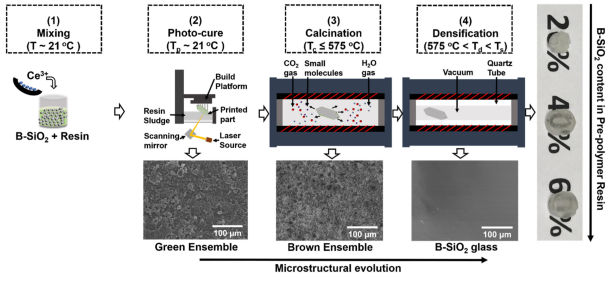

Figure 18: Schematic of the SLA process for glass, from the resin slurry preparation to the final sintered part.[19]

18 Photoresist-Silica Slurry

The creation of a suitable silica-photoresist mixture called "slurry," is the first step. It begins with a "photoresist": a photopolymer typically containing monomers, oligomers, and a photoinitiator. The key modification is the incorporation of silica particles into this organic matrix. To achieve a high-quality final glass part, these silica particles must be extremely fine, often on the nano-scale (20-100 nm), to ensure a smooth surface finish and minimize light scattering during printing.

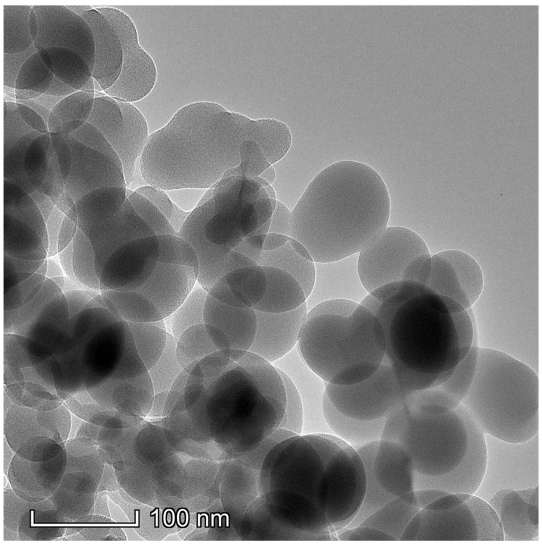

Figure 19: View of the silica spherical particals[20]

The mixing process itself is critical. Simply stirring silica into the resin is insufficient. The goal is a homogeneous and stable suspension where solid silica particles are evenly distributed and do not settle. This often requires specialized techniques like ball milling or ultrasonic mixing to break apart particle agglomerates and ensure each nanoparticle is wetted by the resin. Furthermore, chemical surface modifiers, or coupling agents, are frequently added. These agents coat the silica particles, improving chemical compatibility with the organic resin, which enhances stability and reduces viscosity by preventing particle clumping.

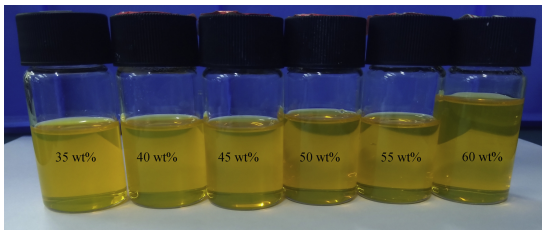

Figure 20: Slurry preparation with different silica weight percentage[20]

The weight percentage of silica is a pivotal parameter. A higher loading (typically 40-60 vol%) is desirable as it increases the density of the final sintered glass part and reduces shrinkage and potential deformation during debinding. However, this advantage comes with a challenge: viscosity. As the weight percentage of solid silica increases, the viscosity of the resin rises dramatically. This high viscosity is the primary limiting

factor for using standard SLA or DLP hardware, which are designed for low-viscosity liquids that can be easily recoated into a thin, uniform layer. A highly viscous silica-loaded resin flows poorly, leading to challenges in recoating, which can result in failed prints, layer delamination, and inconsistent cure depth. This viscosity also impacts the mechanical properties of the intermediate "green" part; a resin with a higher, well-dispersed solid loading can result in a stronger "green" part, which is crucial for surviving post-printing handling. The entire formulation is a delicate balance between maximizing silica content for good final properties and managing viscosity for printability.

19 Post Processing: Debinding and Sintering

The debinding and sintering processes represent the critical thermal transformation stages that convert the fragile, polymer-based green part into a solid glass object. These are not simple heating steps but are calibrated thermal cycles performed in a controlled atmosphere furnace.

The Debinding Process: The debinding process is the first and most delicate thermal stage. The temperature is slowly raised to a medium range, typically between 400°C and 600°C, with a very slow heating rate of 0.5-2°C/min. The primary goal is the complete removal of the organic polymer matrix. Heating too quickly causes the polymer to decompose rapidly, generating gases that can blister, crack, or violently rupture the delicate silica structure from within. A successful debinding, which can take 12-48 hours, results in the "brown part". A pure but porous and fragile scaffold of fused silica nanoparticles that retains the original geometry.

The Sintering Process: Following debinding, the sintering process takes place at a significantly higher temperature, generally between 1250°C and 1350°C for silica. During sintering, the primary physical mechanism is viscous flow. The intense heat causes the surfaces of the silica nanoparticles to soften, and surface tension drives the particles to flow together, coalescing to reduce their total surface area. This action eliminates the pores present in the brown part, leading to significant, isotropic shrinkage of the object (typically 20-30% linearly) and its densification into a solid monolith.

The degree of shrinkage is highly dependent on the initial solids loading of the slurry. A higher silica content in the green part results in less volumetric shrinkage during sintering, as there is less porosity to remove. This relationship must be accounted for in the initial design phase through scaling of the digital model. The major challenge in sintering is to control this shrinkage uniformly via a carefully controlled heating rate (1-5°C/min) and soaking time (1-4 hours) to prevent warping, distortion, or the formation of internal cracks.

The results of these thermal processes directly define the final object's properties. A successfully sintered part is fully dense, leading to mechanical properties (hardness, fracture toughness) that can approach those of commercial fused silica. However, any residual porosity or micro-cracks will severely weaken the component. The optical properties are equally dependent on the process outcome. To achieve high transparency, sintering must be nearly perfect, eliminating all light-scattering pores. Any remaining porosity results in a translucent or opaque material. The primary limitation of this entire two-stage thermal process is the inherent difficulty in precisely controlling the complex shrinkage and preventing deformation, which currently restricts the maximum size and geometric fidelity of parts that can be reliably produced.

Those two time consuming steps represent one of the challenges and area of possible improvement of the process. It was for instance tried to use pressureless spark plasma sintering (PL-SPS) instead of the conventional pressureless sintering which resulted in a reduction of the sintering to less than an hour ![21] Of course the use of this relatively new and very expensive method may not be applicable yet but highlights efforts made to speed up the post processing stages.

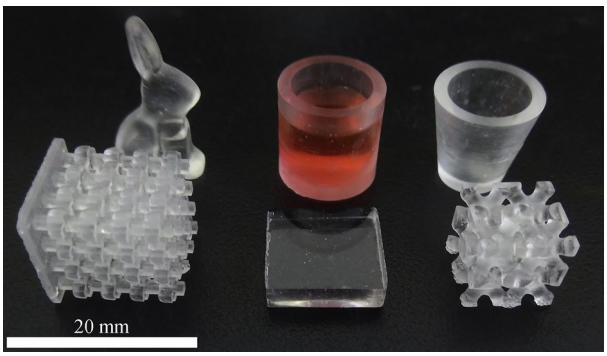

Figure 21: 3D printed glass samples with complex shapes[20]

Mechanical properties The mechanical properties of glass fabricated via Stereolithography (SLA/DLP) are primarily governed by the final density and microstructure achieved after sintering. While the mechanical integrity of the final sintered glass is critical for applications, a systematic investigation of mechanical properties like Young's modulus and fracture toughness is not the primary focus of most found studies on silica-based SLA/DLP. These works often prioritize demonstrating geometric feasibility, optical transparency, and process parameters. For instance some limited themseflves to a Vickers hardness test[20] showing similar hardness to that of fused silica.

The study by [22] provides a benchmark for a high-performance glass-ceramic, specifically lithium disilicate, which is distinct from the pure fused silica often discussed in other works. They reported a biaxial bending strength of up to 431 MPa for polished samples printed with a 25 µm layer thickness, a value that surpasses many conventional pressed lithium disilicate ceramics. Furthermore, the high reliability of their process was demonstrated by a Weibull modulus of 11.5 for 'as-fired' parts, indicating a consistent flaw distribution and high structural integrity.

However, these results are specific to the lithium disilicate glass-ceramic system and its optimized post-processing. The study highlights a critical process-specific finding: samples printed with a 50 µm layer thickness showed a significantly lower average bending strength (263 MPa), underscoring that printing layer thickness is a critical parameter influencing mechanical performance, likely due to defect size or phase separation effects during printing. For fracture toughness, they estimated a value of $\widehat{2.96}$ MPa·m$^{0.5}$ via Vickers indentation, which is consistent with the known properties of this specific glass-ceramic but does not provide a direct measure of the fracture toughness for pure silica glass. In summary, this work proves that SLA/DLP can produce glass-ceramic parts with mechanical properties matching or exceeding those of traditionally manufactured counterparts, but it also emphasizes that the outstanding values for strength and Weibull modulus are intrinsically linked to the specific material (lithium disilicate) and an exceptionally well-controlled process chain. The significant (20-30%) and potentially anisotropic shrinkage during sintering can also introduce internal stresses if not perfectly controlled, which may locally weaken the final part.

20 Applications

Stereolithography for glass finds applications in several domains where high resolution and complex geometry are paramount:

- **Micro-optics:** Complex lens arrays, waveguides, and free-form optical elements.
- **Microfluidics:** Lab-on-chip devices with intricate internal channel networks.
- **Biomedical:** Customized implant, dental for instance[22], with desired optical property.
- **Art and Design:** Sculptural elements with high geometric complexity.

21 Advantages and Limitations

21.1 Advantages

- **Exceptional Resolution:** Capable of producing features down to $\sim$10 μm.
- **Superior Surface Finish:** Offers the best surface quality among glass AM technologies.
- **Geometric Freedom:** Enables complex geometries with overhangs, internal features, and undercuts.
- **Compatible with commercial printers:** although it presents challenges with slurry viscosity and abrasion

21.2 Limitations

- **Extensive Post-Processing:** Requires time-consuming (typically 1-3 days) and energy-intensive debinding and sintering.
- **Size Limitations:** Restricted build volume due to printer technology
- **Material Challenges:** High-viscosity slurries are difficult to handle and expensive.
- **Shrinkage and Deformation:** Significant (25-35%) and anisotropic shrinkage during sintering complicates dimensional control.
- **Fragile Intermediates:** Green and brown parts are very delicate, complicating handling.

21.3 Future Developments

Future developments for glass stereolithography are focused on overcoming current limitations and expanding its capabilities. Key research directions include formulating advanced slurries with higher solid loading and lower viscosity to improve printability, and implementing more sophisticated process control through better sintering protocols and shrinkage prediction models to enhance dimensional accuracy. A major goal is to drastically reduce the post-processing time for debinding and sintering, thereby improving the overall production cadence. Furthermore, efforts are underway to expand the material palette beyond pure silica to include other technical glasses like borosilicates and phosphates, and to pioneer multi-material printing to create functionally graded glass components within a single build.

Part IV

Processes for crystalline materials and micro-industry

22 Overview of the processes

It would be possible to end our report here, however by doing so we would overlook a large part of the processes involving crystalline materials. Eventhough they do not share the share the same micro structure (glass having an amorphous crystal structure), glass and crystalline materials have more in common than one would initially think. From their density to their thermal and mechanical properties they are similar in every way and allow for a great range of processes and applications. For theses reasons it was relevant to include them in our report.
In this section we will present three key processes used in micro-industry and coating fabrication: the Czochralski method for single-crystal silicon wafer creation, the Physical Vapor Deposition (PVD) method for thin-film deposition on silicon substrates, and the Atomic Layer Deposition (ALD) technique for ultra-thin conformal coatings.

22.1 Czochralski method

The Czochralski method is used to grow a large, single-crystal silicon ingot from molten silicon, which is then sliced into wafers used as the base substrate for micro/nano-fabrication.

The processing steps are the following : First very pure polycrystalline silicon chunks are gathered as the source material. Optionally dopants can be used as well. Then the silicon is melted in a quartz crucible inside a high-temperature furnace around 1420 °C under inert atmosphere typically composed of argon. This inert atmosphere will ensure that no undesired oxidation occurs during the melting When the entirety of the source material is molten, a single-crystal silicon seed is dipped into the melt; it defines the crystal orientation and initiates growth.

Figure 22: Initial seeding [23]

The seed is slowly pulled upward and rotated a few millimeters per minutes so that silicon atoms solidify onto the seed lattice and extend the single crystal downward into the ingot. The rotation ensures temperature and composition uniformity inside the final ingot [24].

Figure 23: Necking stage [23]

When the crystal is initially pulled a necking stage, characterized by the thin diameter of the ingot, is used. The purpose of the necking stage is to reduce dislocations and defects. Then the diameter is increased to form the main cylindrical ingot. The diameter is controlled by pulling rate and temperature gradient meaning that a faster pull will lead to a smaller diameter. Typically, the pull rate is between about 0.40 mm/minute to about 1.50 mm/minute during the growth of the main body of the crystal [25]. After growth, the crystal is slowly cooled to avoid internal stresses and cracking. The typical values for dislocations and defects density range from 1×10^3 defects/cm^2 [26]. For defects larger than 10 µm in size, the density falls to 10 defects/cm^2 [27].

Once the ingot is created it undergoes mandatory post-growth processing in order to make it suitable for

use. The ingot is first Trimmed and grinded, the conical ends and irregular parts are cut off, and the ingot is ground into a precise cylinder.

Then, using a diamond wire saw the cylindrical ingot is sliced into thin wafers around 200 µm to 1000 µm thick. Finally the wafers are lapped, etched, and mirror-polished to achieve an atomic-level flatness and prepare the surface for further microfabrication [24]. Although this method is rather energy consuming due to the melting of the silicon, it allows for a small cost of production thanks to the high repeatability and dense production rates. For instance the lowest cost achievable is arround 26 CHF/m^2 [28]

22.1.1 Parameters and control

In the Czochralski method, the key parameters are temperature, pulling rate, and rotation. The silicon must be kept just above its melting point, around fourteen hundred degrees Celsius. A few degrees too high and the melt becomes unstable, creating convection currents that disturb uniformity. A few degrees too low and the crystal front solidifies unevenly, trapping defects. The temperature gradient between the melt and the solid crystal is just as critical. If it is too steep, thermal stress builds up and cracks may appear; if it is too shallow, the interface can become unstable.

Moreover the pulling rate defines how fast atoms arrange themselves into the crystal lattice. Pulling too slowly might cause inefficient production, whereas pulling too quickly is likely to cause dislocations and stresses. The rotation of both the crystal and the crucible helps mix the melt, spreading dopants evenly (if added). Doping control is another key aspect: tiny variations in dopant concentration can shift resistivity, which directly affects how chips behave later on.

Even after growth, the cooling rate matters critically. The crystal must cool slowly enough to avoid stress, but fast enough to prevent oxygen precipitation. Each of these parameters connects directly to wafer quality. The better they are balanced, the more uniform and reliable the final silicon becomes.

22.2 Physical Vapor Deposition (PVD) for silicon and silicates

PVD refers to a family of vacuum-based techniques in which a solid source material is vaporised and then deposited onto a substrate, forming thin films of amorphous silica or silicate films on silicon or other substrates. It is widely used for thin-film coatings rather than bulk substrates.

The porcess happens in the following order : First, a solid source material (SiO_2 or silicate) inside a vacuum chamber is heated via thermal evaporation, electron beam heating, or bombarded by ions to generate atoms or molecules in the vapour phase. Then, the vapour containing the atoms travels through a medium to high vacuum environment toward the substrate, The movement of the particle vapour is driven by the pressure differential between the source and the substrate. The role of the vacuum in this step is to reduce collisions and contamination so atoms reach the substrate almost in straight lines. Finally the vapour arrives to the substrate, sticks to its surface and condense into a solid film. [29]

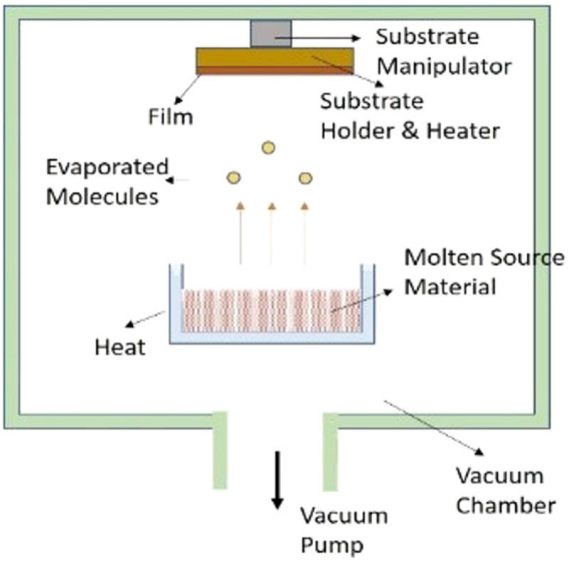

Figure 24: PVD process overview [30]

Unlike the Czochralski method, the post treatment is not mandatory for this method. However after deposition, the film may be annealed or densified to relieve stress, improve adhesion, remove defects or adjust composition.

22.2.1 Parameters and control

In PVD the thickness is controlled by deposition time and rate; uniformity is affected by substrate geometry, substrate rotation, and vacuum conditions. Because deposition is largely line-of-sight, film coverage on complex 3D or high-aspect-ratio structures may be limited due to shadowing effects, unless special geometry or rotation is used.

In PVD, the whole process is related to how atoms move through vacuum and land on a surface. The chamber pressure is the main actor for that matter, low pressure means atoms travel in straight lines, creating clean, dense films. If the pressure rises, atoms scatter, the film becomes rougher, and impurities appear. In addition the energy used to vaporize the target material also matters. In sputtering, for example, too much energy can damage the growing surface, while too little leaves weak, porous films.

The temperature of the substrate during deposition is also a major factor for the final microstructure [31]. At low temperatures, atoms stick where they land, forming loose columns. On the other side if temperature is too high, the roughness of the surface increases as a consequence to the increase in the surface diffusion length [32]. The deposition rate is not really a parameter that you can control directly through a command but rather a consequence of the rate of atom vaporization, for instance the deposition rate varies from 0.1 to 100 µm/min depending on the method of vaporization [33].

Uniformity is the main flow of PVD. Because deposition is line-of-sight, shadowed areas receive less material, especially on complex geometries. Substrate rotation and clever source design can help, but there is always a trade-off. Finally, post-deposition annealing can refine the film, improving adhesion and density.

22.3 Atomic Layer Deposition (ALD) for silicon / SiO_2 films

ALD is a vapor-phase thin film technique that builds materials one atomic layer at a time through self-limiting surface reactions, enabling excellent thickness control, highly conformal coatings even on complex 3D structures, and uniform film properties. However the excellent conformity and uniformity comes with a cost, this process is very slow and produces a deposition rate between 0.05 and 0.15 nm/cycle [34].

The ALD process happens over incremental iterations each divided in four main steps. First, a gaseous silicon-containing precursor such as $SiCl_4$ is pulsed into the reaction chamber; it bonds to active surface sites (–OH, $–NH_2$) on the substrate. The key information is that the reaction of bonding only stops once there are no active surface sites (because the surface sites molecules are the limitant reactive species), this means that when exposed long enough, the whole surface is covered with the precursor gas and ready for the next step.

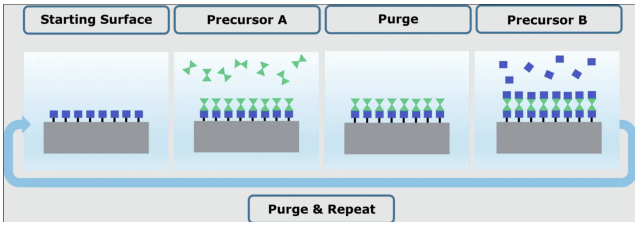

Figure 25: ALD process overview [35]

Once the precursor exposure is done an inert gas (N_2 or Ar) flushes out excess precursor and by-products. This allows for a clean and inert atmosphere between each step. Then a reactant such as H_2O, O_3 or NH_3 is pulsed in; it reacts with the adsorbed precursor layer, forming the final solid material and regenerating surface groups for the next cycle. When the reaction is over the environment is purged again to remove remaining reactant and clean the atmosphere for the next cycle Finally, once one cycle is over and one layer of infinitesimal thickness is created the process can repeated any number of times needed. It isimportant to note that majority of the time elapsed per cycle is due to the purges, indeed, whereas the time of exposure is at least one second depending on the precursor, the time of purge is at least five seconds. For the majority of cases the exposure and purge time are much longer to ensure maximum reaction with the surface [36] [37].

22.3.1 Parameters and control

Film thickness is directly controlled by the number of ALD cycles. The self-limiting reactions and alternating pulses allow full coverage even on high-aspect-ratio trenches or porous substrates. The film quality is elite, dense, pinhole-free, because interfaces and defects can be managed at the atomic scale.

The ALD process relies on alternating doses of precursor and reactant gases, each reacting only with the surface until it is fully covered. The substrate temperature has to sit high enough to drive the reactions, but low enough to prevent unwanted chemical vapor deposition. Pulse duration and purge times are key parameters of ALD. If the pulses are too short, not all sites react; if they are too long, the extra time adds nothing but slows production. Purging too briefly leaves behind byproducts that can cause unwanted reactions; too long and throughput drops [37]. Chamber pressure and gas flow define how evenly the precursors reach every corner of the substrate, which is especially important for high-aspect-ratio structures.

Because each cycle deposits only a fraction of a nanometre, uniformity depends on consistency and requires identical conditions for each cycle.If the conditions are met the result is exceptional precision and conformality, even on complex 3D geometries.

23 Results and Applications

23.1 Application Domains

For the Czochralski method there is only one main application since the method was created specificaly for the micro-chip industry .

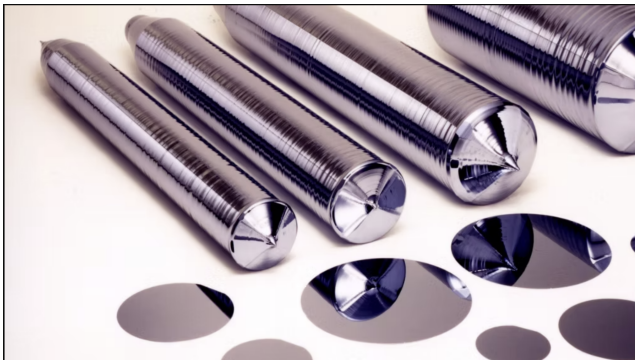

Figure 26: Final waifer [38]

Wafers produced via the Czochralski method serve as the foundational substrate for essentially all modern integrated circuits in microprocessors, memory chips, sensors and for monocrystalline silicon solar cells.

Example applications for PVD-deposited thin films include optical coatings, anti-reflection coatings, protective coatings, waveguides, barrier/packaging films, protective and dielectric coatings in MEMS/NEMS devices, and thin metal/ceramic films in optoelectronics and electronics.

Typical uses of ALD silicon/SiO_2 films are very broad due to the excellent conformity of the coatings. It is often used in gate dielectrics and spacer oxides in microelectronics but also conformal insulating or passivation coatings on micro/nano-mechanical structures, anti-reflective or protective silica layers [39], passivation for energy devices, solar cells, batteries, and biocompatible or corrosion-resistant coatings on nanostructures.

23.2 Limitations

Allthough the Czochralski method requires high capital cost and energy consumption due to melting large amounts of silicon, slow pulling rates and strict control of thermal gradients, since it produces high volume of materials (hundreds of chips per waifer and hundreds of waifers per ingot) it is considereed very efficient and econoùically substainable. In fact the tendency is to increase the diametter in order to produce more chips and get better profitability of of each ingot. A flow of the Czochralski method is the potential for oxygen and carbon contamination especially from quartz crucible contact and associated defects, especially compared with other methods like float-zone. Finally the process is inherently batch and limited in flexibility; large wafer sizes pose increased mechanical and thermal stress and have not yet been universally adopted even though they inevitably will.

The main limitation of PVD resides in the method of deposition it self, the "Line-of-sight deposition" makes the coating of trenches, high-aspect-ratio structures or shadowed regions, very uneven. Natyrally, vacuum system are complex and their cost is non-negligible. Since the method does not rely on any types of thickness or cycle control, controlling film stress, adhesion and contamination can be challenging and approximate.

ALD beeing more precise, it evidently comes with some drawbacks; the process allows for lower deposition rates and hence lower throughput compared to other deposition methods, which can limit production volume or increase cost. Equipment and precursor cost can be high; precursor availability, precursor purity and choice of chemistry especially for SiO_2 may introduce impurities or long cycle times. While excellent in conformality, ALD may not always match the high deposition rates needed for thick films, so it's typically used for thin coatings rather than bulk layers.

24 Comparative Perspective

In terms of production volume and scalability, the Czochralski process is highly scalable for wafer substrate production, capable of producing industrial-scale wafers several hundred millimetres in diameter. Physical Vapor Deposition is also very scalable for thin-film deposition across many wafers per batch, though its throughput can be limited by vacuum cycle times and the required film thickness. Atomic Layer Deposition , meanwhile, offers excellent uniformity and conformality, but its slower deposition rate restricts throughput for thick films, making it best suited for high-precision, lower-volume, or specialized coatings.

Regarding precision, film quality, and coverage, Czochralski growth produces high-quality single-crystal silicon wafers with uniform crystal orientation and low defect levels when well controlled. PVD provides good film quality for numerous applications, though its coverage on complex geometries is limited and its atomic-scale thickness precision is lower than that of ALD. By contrast, ALD achieves superior precision with sub-nanometre thickness control and excellent conformality over complex geometries, making it ideal for advanced micro- and nanostructures.

When it comes to energy use, equipment intensity, and cost, the Czochralski method requires very high temperatures, large crucibles, and long growth cycles, leading to high energy consumption and capital costs.However if we contrast this cost with the volume of production this method allows, we can conclude it is economically sustainable. PVD, while dependent on high vacuum and high-energy deposition techniques such as sputtering or evaporation, is generally less extreme in terms of cost than crystal growth but still involves substantial equipment expenses (up to 3 million dollars for top end PVD system)[40]. ALD relies on

specialized precursor delivery systems and tightly controlled chambers; although deposition temperatures and energies can be moderate, the cost per unit area tends to be higher for thicker films.

Considering application domain suitability, the Czochralski process is ideal for producing substrates such as wafers used in electronics, MEMS, and solar cells. PVD is best applied to thin coatings—optical, protective, barrier, or metallic—especially for relatively planar geometries. ALD excels in cases where atomic-scale control and conformality are critical, such as in high-aspect-ratio or three-dimensional microstructures, advanced passivation layers, and nano-coatings.

Finally, in terms of limitations and trade-offs, Czochralski growth involves balancing wafer size and growth speed against defect control, with larger diameters introducing greater mechanical stress and cost. PVD faces a trade-off between deposition speed and uniformity, particularly over complex geometries. ALD, on the other hand, trades its ultimate precision and conformality for slower deposition rates and higher costs when producing thick films

25 Concluding Remarks

In summary, the three processes each play distinct roles in micro-industry and coating industry : the Czochralski method provides the foundational substrate material; PVD enables many of the thin film coatings needed for functional layers; and ALD offers the highest precision coatings for advanced device architectures. Choosing among them or combining them depends on required film thickness, geometry, precision, throughput and cost. Understanding their process steps, control considerations, applications and limitations is essential for designing and manufacturing next-generation micro-devices and chips.

Part V
Summary of main quantities

Parameter	Fused Deposition Modeling
Resolution [μm]	4000-6000
Build Volume	Large (Architectural Scale)
Material	Molten Soda-Lime Glass
Build Speed	Slow (Layering + Cooling)

Table 1: Parameters of Fused Deposition Modeling for glass

Parameter	Laser Powder Bed Fusion
Resolution [μm]	$\sim$50-1100
Build Volume [mm]	from 200x200x300 to 700x380x560
Material	Soda-Borosilicate or Soda-Lime Glass Powder
Build Speed	Slow (Powder Recoating + Laser Scanning)

Table 2: Parameters of Laser Powder Bed Fusion for glass

Parameter	Stereolithography
Resolution [μm]	x-y: 25 to 100 / z: 25 or 50 (curing depth)
Build Volume [mm]	50 x 50 x 200
Material	Photoresist and Silica Slurry
Build Speed	Slow (Printing + Days of Post-Processing)

Table 3: Parameters of Stereolithography for glass

Parameter	ALD
Resolution [μm]	x-y: 25 to 100 / z: 25 or 50 (curing depth)
Build Surface [mm]	1000 x 1000
Build Speed	Very Slow (Printing + Days of Post-Processing)

Table 4: Parameters of Stereolithography for glass

26 Conclusion

This review has presented an overview of recent advances in additive manufacturing applied to glass and has shown that, while still a young and slowly evolving research field, it holds great promise. The processes investigated exhibit strong potential for applications across diverse sectors such as architecture, art, optics, and healthcare, where they could provide an efficient and flexible means of prototyping complex structures unattainable or time and cost expensive with conventional methods.

Fused Deposition Modeling demonstrates that, despite numerous technical challenges, transparent and large-scale glass objects can be fabricated directly from melting glass, effectively bridging traditional craftsmanship with digital design.
Laser Powder Bed Fusion, encompassing both Selective Laser Sintering and Selective Laser Melting, enables the production of intricate geometries while preserving the chemical inertness of glass, though optical transparency and mechanical strength remain limited by porosity and thermal stresses.
Stereolithography achieves unparalleled resolution and surface quality, making it particularly suitable for micro-optical and biomedical components, at the expense of extensive post-processing and restricted build volume.

Overall, while these technologies remain primarily at the research stage, they have already demonstrated remarkable potential. With continued developments in glass material formulation, process control, and post-treatment, glass additive manufacturing could become a key technology for future design and engineering applications.

As demonstrated during this review, the domain of additive processes for glass materials is much broader than it looks, although glass is an amorphous material, other materials with crystalline compositions were included in this review because of their similar physical aspect, their close material properties and interactions with the environment. The three techniques concerning crystalline materials that we reviewed are different in many ways with the previous ones mentioned, they often act at micro-scale and are much slower. In the mean time they are more precise than other methods and play an important role in the micro-industry, coating industry and micro-chip industry. They each posses crucial properties, from the high volume and high repeatability of the Czochralski method to the atomic level precision of the ALD method, which are impossible to bypass in todays industry.

27 Outlook

This review has highlighted the key challenges and future research required to make glass additive manufacturing a reliable, efficient, and scalable technology. Despite the remarkable progress achieved in recent years, significant efforts are still needed to overcome the limitations currently preventing its large-scale use.

- **Scalability and reproducibility:** Improving the scalability of glass AM processes is essential to enable the fabrication of larger parts with consistent quality. This requires a deeper understanding and control of process parameters to ensure repeatable results across builds.
- **Material feedstock development:** Further studies are needed to identify and optimize glass compositions with suitable viscosity, laser absorptivity, and thermal stability. Finding the right feedstock composition could improve densification, transparency, and mechanical strength of the glass parts.
- **Optical clarity:** Achieving and maintaining optical transparency remains one of the most challenging objectives. Hence, significant progress in the process control and the thermal management will be required for applications where transparency is critical, such as optics.
- **Post-processing optimization:** Further research in postprocessing methods is needed as it offers promising opportunities in improving aesthetic, optical and mechanical properties of the produced parts.
- **Mechanical characterization:** There is a crucial need for systematic mechanical testing of additively manufactured glass, as current data remain rare. A thorough understanding of the relationship between process parameters, porosity, and mechanical strength is central to the reliable use of printed glass components.
- **Thermal behavior during printing:** Detailed investigation of the thermal gradients and heat transfer phenomena occurring during the manufacturing processes are required as it currently limits process stability, scalability, and overall part quality.

In the future, glass additive manufacturing could evolve from an emerging research topic into a key technology, allowing for rapid and flexible production of complex, customized glass components. However, a lot of additional research effort is needed as many challenges remain and progress is still very slow.

As for the future of the methods concerning crystalline, active research is still very much needed in this domain as there are still problems to solve like :

- **Deposition rate :** The main flow of micro-scale deposition methods is that their deposition rate is very slow. This due to the fact that often the methods operate via single molecule deposition which inherently leads to high film density and uniformity but comes with the cost of very low deposition rate.
- Simple geometry of The PVD method only works with relatively simple geometries, hence there is a need to find ways to extend this method to more complexe geometries as it would be beneficial in many applications like ...

References

[1] D. Patchen and Wikimedia Commons contributors. "Cane foglio — david patchen." Photograph of a glass artwork by David Patchen, available on Wikimedia Commons under a Creative Commons license (CC BY-SA 3.0). [Online]. Available: https://commons.wikimedia.org/wiki/File:Cane_Foglio_-_David_Patchen.jpg.

[2] C. Xin, Z. Li, L. Hao, and Y. Li, "A comprehensive review on additive manufacturing of glass: Recent progress and future outlook," *Materials & Design*, vol. 227, p. 111 736, 2023, Comprehensive review summarizing recent advances, energy implications, and industrial prospects of glass additive manufacturing technologies. DOI: 10.1016/j.matdes.2023.111736. [Online]. Available: https://doi.org/10.1016/j.matdes.2023.111736.

[3] N. Oxman et al., "Additive manufacturing of optically transparent glass," *3D Printing and Additive Manufacturing*, vol. 2, no. 3, pp. 92–105, 2015. [Online]. Available: https://cdn.prod.website-files.com/67a0e71b585471299b7a71e9/67d85ef0a6dfea5e021259df_Additive-Manufacturing-of-Optically-Transparent-Glass-(2015).pdf.

[4] J. Klein et al., "Methods and apparatus for additive manufacturing of glass," Patent US10266442B2, Apr. 2019. [Online]. Available: https://patents.google.com/patent/US10266442B2/en.

[5] F. News. "Glass 3d printing (g3dp)." News article presenting the MIT Media Lab's G3DP glass 3D printing project. [Online]. Available: https://futuristicnews.com/glass-3d-printing-g3dp/.

[6] M. M. Lab. "G3dp ii: Glass 3d printing for architectural scale." Official MIT Media Lab project page describing the second generation of the G3DP system for large-scale glass 3D printing. [Online]. Available: https://www.media.mit.edu/projects/g3p-ii/overview/.

[7] M. G. Printing. "Equipment — maple glass printing." Commercial equipment developed from the MIT G3DP research on additive manufacturing of glass. [Online]. Available: https://www.mapleglassprinting.com/equipment.

[8] S. Koppka, B. Oberleiter, T. I. Kwinda, M. Steimecke, and D. Enke, "Fabrication of 2d and 3d shaped controlled porous glasses via selective laser sintering and its effect on glass structure and microstructure," *Journal of Manufacturing Processes*, vol. 93, pp. 173–192, 2023. DOI: https://doi.org/10.1016/j.jmapro.2023.02.054.

[9] F. Klocke, A. McClung, and C. Ader, "Direct laser sintering of borosilicate glass," in *Proceedings of the 2004 International Solid Freeform Fabrication Symposium*, 2004. DOI: 10.26153/tsw/6986. [Online]. Available: https://hdl.handle.net/2152/79961.

[10] Wikipedia contributors. "Borosilicate glass." Accessed: 11 November 2025, Wikipedia, The Free Encyclopedia. [Online]. Available: https://en.wikipedia.org/wiki/Borosilicate_glass.

[11] K. C. Datsiou, F. Spirrett, I. Ashcroft, M. Magallanes, S. Christie, and R. Goodridge, "Laser powder bed fusion of soda lime silica glass: Optimisation of processing parameters and evaluation of part properties," *Additive Manufacturing*, vol. 39, p. 101 880, 2021. DOI: 10.1016/j.addma.2021.101880.

[12] M. Fateri, A. Gebhardt, S. Thuemmler, and L. Thurn, "Experimental investigation on selective laser melting of glass," *Physics Procedia*, vol. 56, pp. 357–364, 2014. DOI: 10.1016/j.phpro.2014.08.113.

[13] Wikipedia contributors. "Soda–lime glass," Wikipedia, The Free Encyclopedia. [Online]. Available: https://en.wikipedia.org/wiki/Soda%E2%80%93lime_glass.

[14] M. Shaw et al., "The additive manufacturing of glass: A critical review," *Applied Sciences*, vol. 15, no. 5, p. 3414, 2025. DOI: https://doi.org/10.3390/app15063414.

[15] R. D. Goodridge, K. W. Dalgarno, and D. J. Wood, "Indirect selective laser sintering of an apatite–mullite glass–ceramic for potential use in bone replacement applications," *Proceedings of the Institution of Mechanical Engineers, Part H: Journal of Engineering in Medicine*, vol. 220, no. 1, pp. 57–68, Jan. 2006. DOI: 10.1243/095441105X69051.

[16] L. Haferkamp et al., "The influence of particle shape, powder flowability, and powder layer density on part density in laser powder bed fusion,"

Metals, vol. 11, p. 418, 2021. DOI: https://doi.org/10.3390/met11030418.

[17] S. Ziegelmeier et al., "An experimental study into the effects of bulk and flow behaviour of laser sintering polymer powders on resulting part properties," *Journal of Materials Processing Technology*, vol. 215, pp. 239–250, 2015. DOI: 10.1016/j.jmatprotec.2014.07.030.

[18] T. Yang, Z. Feng, Y. Qiu, W. Han, and L. Kong, "Selective laser melting of glass with irregular shaped powder," *Journal of Materials Research and Technology*, vol. 23, pp. 2503–2522, 2023. DOI: https://doi.org/10.1016/j.jmrt.2023.09.047.

[19] O. Okpowe, V. Drozd, O. Ares-Muzio, N. Pala, and C. Wang, "Additive manufacturing of borosilicate glass via stereolithography," *Ceramics International*, vol. 48, no. 9, pp. 12 721–12 728, 2022. DOI: https://doi.org/10.1016/j.ceramint.2022.01.141.

[20] P. Cai et al., "Effects of slurry mixing methods and solid loading on 3d printed silica glass parts based on dlp stereolithography," *Ceramics International*, vol. 46, no. 10, Part B, pp. 16 833–16 841, 2020. DOI: https://doi.org/10.1016/j.ceramint.2020.03.260.

[21] P. Cai, L. Guo, L. Liu, Q. Zhang, J. Li, and Q. Lue, "Rapid manufacturing of silica glass parts with complex structures through stereolithography and pressureless spark plasma sintering," *Ceramics International*, vol. 48, no. 1, pp. 55–63, 2022. DOI: https://doi.org/10.1016/j.ceramint.2021.08.345.

[22] S. Baumgartner, R. Gmeiner, J. A. Schönherr, and J. Stampfl, "Stereolithography-based additive manufacturing of lithium disilicate glass ceramic for dental applications," *Materials Science and Engineering: C*, vol. 116, p. 111 180, 2020. DOI: https://doi.org/10.1016/j.msec.2020.111180.

[23] Unspecified, "Czochralski crystal growth," 2025. [Online]. Available: http://www.galaxywafer.com/galaxy/technology/crystal-growth/.

[24] G. Villanueva, "Epfl course about the fabrication of micro and nano-mechanical devices," 2025. [Online]. Available: https://moodle.epfl.ch/pluginfile.php/3130415/mod_resource/content/1/2020-08%20-%20Nanofabrication%20ESONN%20-%20Online.pdf.

[25] C. T. Eyles, "Process for controlling thermal history of czochralski-grown silicon," 1998. [Online]. Available: https://data.epo.org/publication-server/rest/v1.2/patents/EP0823497NWA1/document.html.

[26] R. J. F. C. Holzer, "Low defect density silicon," 1997. [Online]. Available: https://patents.google.com/patent/US6287380B1/en.

[27] M. Yamanaka, "Low defect density silicon," 1998. [Online]. Available: Method%20and%20apparatus%20for%20manufacturing%20a%20silicon%20single%20crystal.

[28] M. H. Koliwad K. M Leipold, "Economic analysis of low cost silicon sheet produced from czochralski grown material," 1976. [Online]. Available: https://ntrs.nasa.gov/citations/19780027127.

[29] U. Waseem, "Pvd coating in semiconductors," 2024. [Online]. Available: https://www.wevolver.com/article/pvd-coating-in-semiconductors-a-comprehensive-guide.

[30] Unspecified, [Online]. Available: https://www.researchgate.net/figure/Process-of-physical-vacuum-deposition-PVD_fig6_369723265.

[31] V. Jambur and M. et al., "Temperature effects on the structure and mechanical properties of vapor deposited a-sio," *arXiv preprint arXiv:2204.06103*, 2022. [Online]. Available: https://arxiv.org/abs/2204.06103.

[32] M. R. Amirzada, A. Tatzel, V. Viereck, and H. Hillmer, "Surface roughness analysis of sio for pecvd, pvd and ibd on different substrates," *Applied Nanosci.*, vol. 6, no. 2, pp. 215–222, 2016. [Online]. Available: https://link.springer.com/article/10.1007/s13204-015-0432-8.

[33] Various, "Process for controlling thermal history of czochralski-grown silicon," 2009-2025. [Online]. Available: https://en.wikipedia.org/wiki/Electron-beam_physical_vapor_deposition.

[34] V. Y. Vasilyev, "Atomic layer deposition of silicon dioxide thin films," 2021. [Online]. Available: https://www.researchgate.net/publication/351947147_

Review-Atomic_Layer_Deposition_of_Silicon_Dioxide_Thin_Films.

[35] Unspecified, "What is atomic layer deposition?," 2025. [Online]. Available: https://beneq.com/atomic-layer-deposition/.

[36] Various, "Atomic layer deposition," 2016-2023. [Online]. Available: https://lnf-wiki.eecs.umich.edu/wiki/Atomic_layer_deposition#:~:text=Deposition%20rate%20is%20usually%20expressed%20in%20%C3%85%2Fcycle%20or,self-limiting%20to%20a%20monolayer%20or%20less%20of%20material..

[37] N. A. D. Arl V. rogé, "Sio_2 thin film growth through a pure atomic layer deposition technique at room temperature," 2020. [Online]. Available: https://pmc.ncbi.nlm.nih.gov/articles/PMC9053598/.

[38] Unspecified, [Online]. Available: https://www.powerwaywafer.com/silicon-ingot.html.

[39] H. T. et al., "Atomic layer deposition of silica to improve the high hydrothermal stability of molecular sieve denitrification catalysts," *Applied Catalysis B: Environmental*, 2021. [Online]. Available: https://www.sciencedirect.com/science/article/abs/pii/S0304389421011584.

[40] 24ChemicalResearch. "Global thin-film semiconductor deposition market insights and forecast to 2030." Market research report analyzing global trends, key players, and growth forecasts for thin-film semiconductor deposition technologies. [Online]. Available: https://www.24chemicalresearch.com/reports/148741/thinfilm-semiconductor-deposition-market.